Advanced TOF MLEM reconstruction of a human patient scanned by the modular J-PET

Roman Y. Shopa
National Centre for Nuclear Research
WMLQ 2024

NATIONAL CENTRE FOR NUCLEAR RESEARCH ŚWIERK

Outline

Positron emission tomography

List-mode TOF MLEM with a realistic J-PET system matrix

Single scatter simulation (SSS)

STIR implementation of SSS

SSS for the modular J-PET and normalisation

Scan setup

Results

Ways to improve

Conclusions

Positron emission tomography

$\beta^+ \longrightarrow e^+e^-$ annihilation $\longrightarrow$ 511-keV back-to-back pair

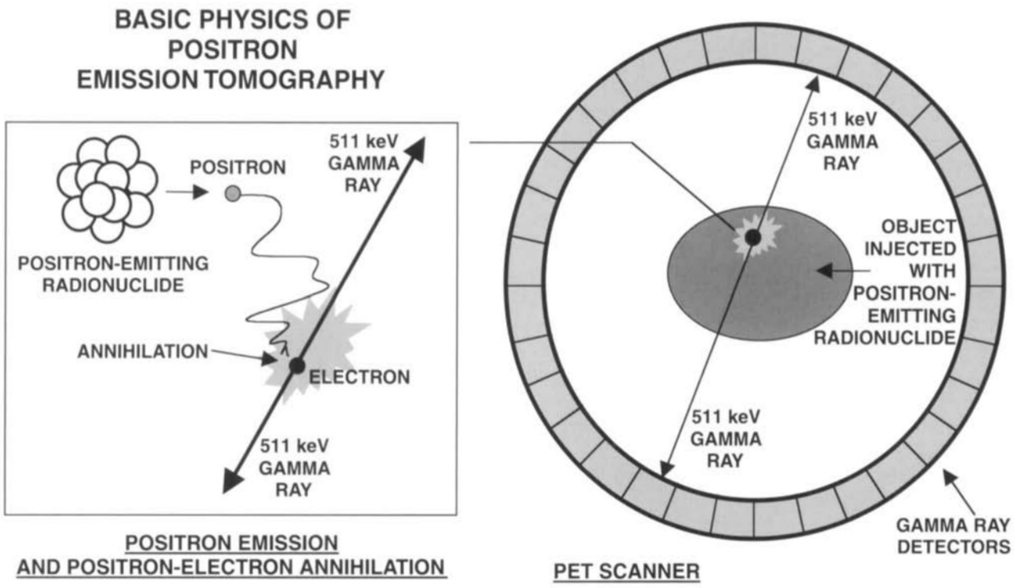

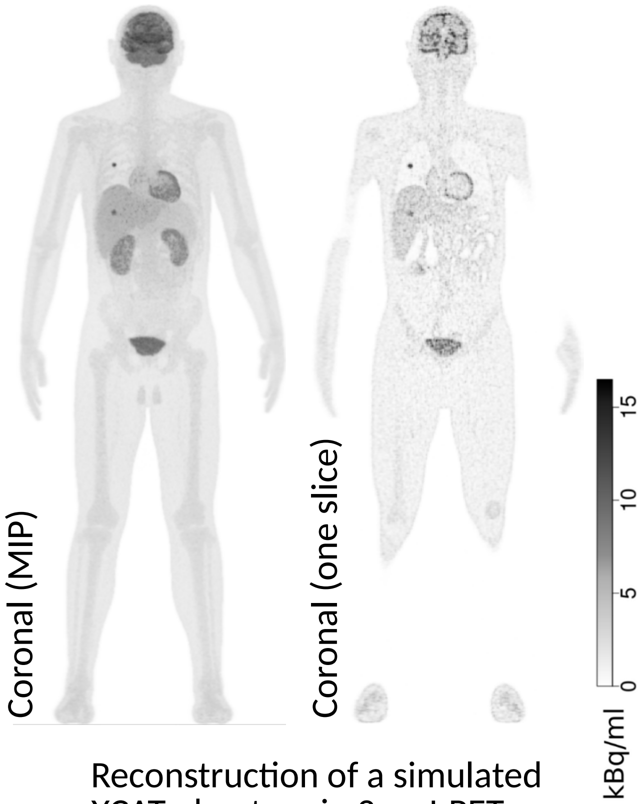

Reconstruction of a simulated XCAT phantom in 2-m J-PET

Fig taken from [S. Cherry, S. Gambhir ILAR Journ 2001]

[Shopa R et al IEEE TRPMS 2023]

Positron emission tomography

Radiotracers: **^{18}F (FDG)** – uptake of glucose (metabolism), **^{15}O** – blood flow, **^{64}Cu-ATSM** – tissue hypoxia, **^{68}Ga DOTATATE** – somatostatin-receptor (SSTR), neuroendocrine tumors

Less used:
^{44}Sc (preclinical cancer),
^{22}Na (long lifetime)

^{22}Na, ^{44}Sc, ^{68}Ga – emit *prompt* photon **(positronium imaging)**

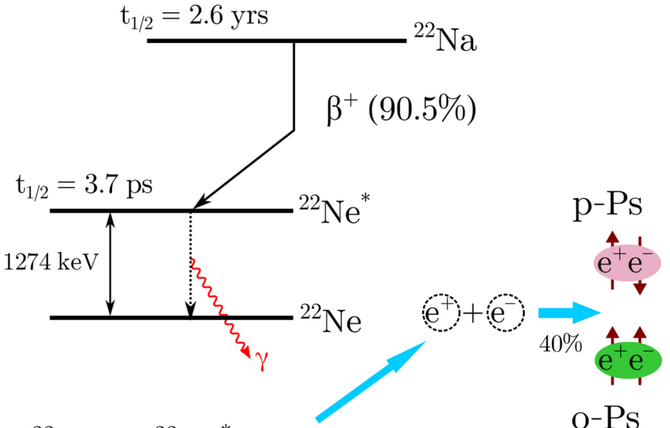

$$^{22}\mathrm{Na} \rightarrow {}^{22}\mathrm{Ne}^* + e^+ + \nu_e$$
$$^{22}\mathrm{Ne}^* \rightarrow {}^{22}\mathrm{Ne} + \gamma_{1274} + e^+ + \nu_e$$

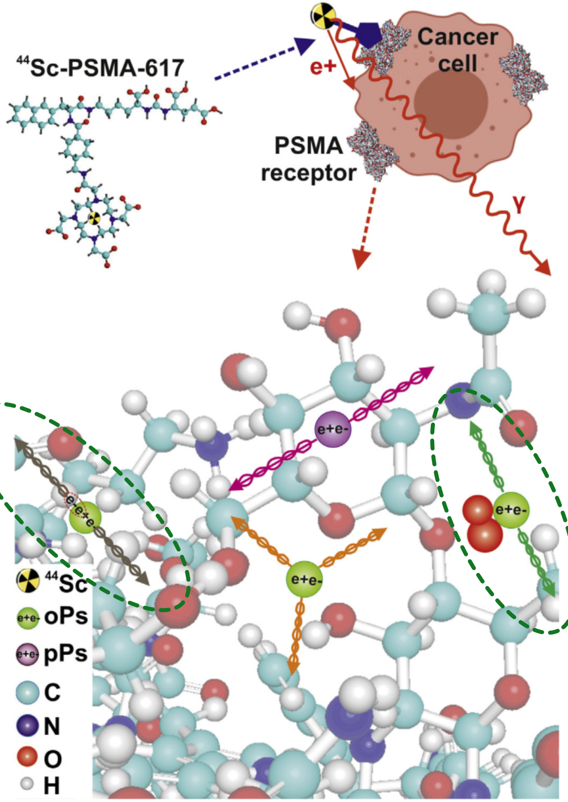

[Moskal Stępień PET Clin 2020]

Maximum likelihood expectation maximisation

The expected (average) data $\langle \mathbf{y} \rangle$ vs an unknown radiotracer distribution $\boldsymbol{\lambda}$ [Lange K. et al. (1984)]:

$$\langle \mathbf{y} \rangle = \mathbf{M}\boldsymbol{\lambda} + \hat{\mathbf{b}}$$

$\mathbf{M}$ – system matrix, $\hat{\mathbf{b}}$ – ***observation error*** (randoms and scatter).
Decomposition of $\mathbf{M}$:

$$\mathbf{M} = \mathbf{M}_{\mathrm{norm}} \mathbf{M}_{\mathrm{det.res}} \mathbf{M}_{\mathrm{att}} \mathbf{M}_{\mathrm{Radon}} \mathbf{M}_{\mathrm{ps.rng}}$$

The measured photon counts $\hat{\mathbf{y}}$ undergo Poisson distribution – a log-likelihood cost function is utilised for MLEM to solve iteratively:

$$\boldsymbol{\lambda}^{(k+1)} = \frac{\boldsymbol{\lambda}^{(k)}}{\mathbf{M}^{\mathrm{T}}\mathbf{1}} \mathbf{M}^{\mathrm{T}} \frac{\hat{\mathbf{y}}}{\mathbf{M}\boldsymbol{\lambda}^{(k)} + \hat{\mathbf{b}}}$$

$\langle \mathbf{y} \rangle$

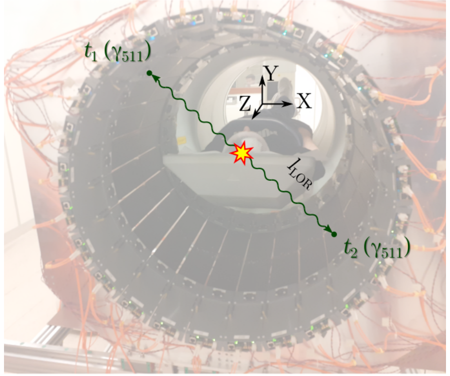

$\boldsymbol{\lambda}$

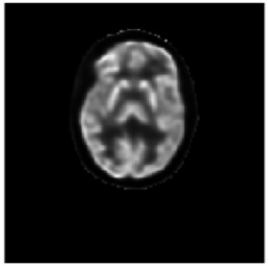

Maximum likelihood expectation maximisation

List-mode MLEM replaces back-projection $\mathbf{M}^{\mathsf{T}}\hat{\mathbf{y}}$ of sinograms with individual events ϵ [Barrett H.H. et al. (1997)]

$$\lambda_j^{(k+1)} = \frac{\lambda_j^{(k)}}{\sum_{i\in\mathcal{I}} m_{ij}} \sum_{\epsilon\in\mathcal{E}} \frac{m_{i_\epsilon,j}}{\sum_{j'\in\mathcal{J}} m_{i_\epsilon,j'}\lambda_{j'}^{(k)} + \hat{b}_{i_\epsilon}}$$

$$\lambda_j \in \boldsymbol{\lambda},\ \hat{b}_{i_\epsilon} = \hat{r}_{i_\epsilon} + \hat{s}_i$$

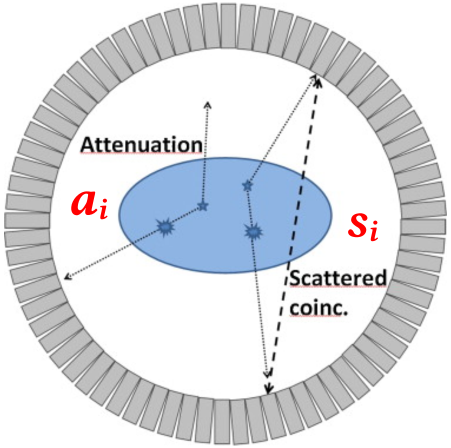

[Martinez-Möller, Nekolla ZMP 2012]

The shift-variant part of M: $m_{ij} = n_i^{\mathrm{cal}} a_i \chi_{ij}$

$a_i \in \mathbf{M}_{\mathrm{att}}$, $\boxed{\chi_{ij} \text{ jointly represents the geometrical part}}$ of $\mathbf{M}_{\mathrm{norm}}$, $\mathbf{M}_{\mathrm{det.res}}$ and $\mathbf{M}_{\mathrm{radon}}$ [Shopa R et al IEEE TRPMS 2023]

List-mode TOF MLEM for Jagiellonian PET

J-PET: plastic scintillators as detectors (Compton scatt.)
Allows ***time-of-flight*** (TOF)!
Requires kernels (H_{TOF}) and ***axial smearing*** (H_Z).

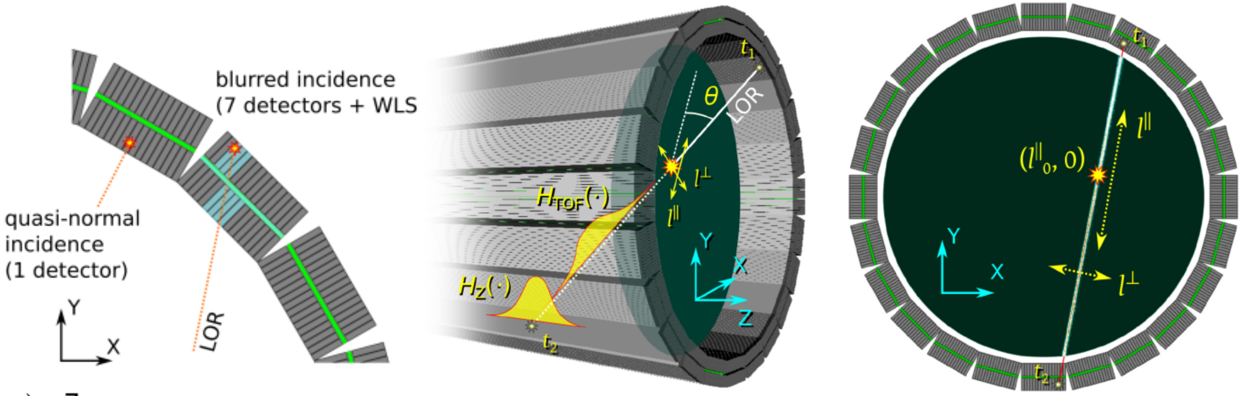

$$\chi_{(it)_\epsilon,j} \rightarrow \chi_{i_\epsilon}\left(l_j^\parallel, l_j^\perp, \theta_\epsilon\right) \cdot H_{\mathrm{TOF}}\left[l_j^\parallel, \left(l_0^\parallel\right)_\epsilon\right] \times \left[H_Z^{\mathrm{CRT}}\left(z_j, l_j^\parallel\right) * H_Z^{\mathrm{prlx}}\left(z_j, l_j^\parallel, i_\epsilon, \theta_\epsilon\right)\right].$$

$$\lambda_j^{(k+1)} = \frac{\lambda_j^{(k)}}{\sum_{i\in\mathcal{I}} n_i^{\mathrm{cal}} a_i \chi_{ij}} \sum_{\epsilon\in\mathcal{E}} \frac{\chi_{(it)_\epsilon,j}}{\sum_{j'\in\mathcal{J}_\epsilon} \chi_{(it)_\epsilon,j'} \lambda_{j'}^{(k)} + \hat{b}_{i_\epsilon}^*}.$$

$$\hat{b}_{i_\epsilon}^* = (\hat{r}_{i_\epsilon} + \hat{s}_{i_\epsilon})/(n_{i_\epsilon}^{\mathrm{cal}} a_{i_\epsilon}) \qquad \forall i \in \mathcal{I}\ n_i^{\mathrm{cal}} = 1$$

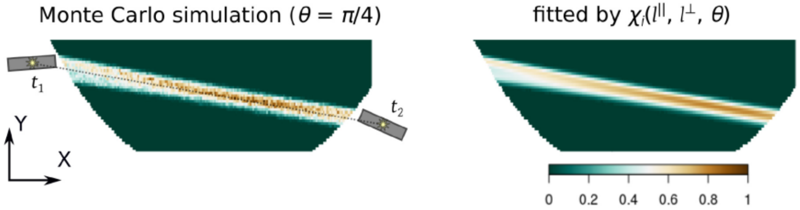

Simulated 2-layer 2-m long J-PET:
χ_{ij} defined via Monte Carlo, then fitted by polynomial [Shopa et al IEEE TRPMS 2023]

List-mode TOF MLEM

Simpler solution (c++): Monte Carlo for a grid $r \times l \times \vartheta_{b2b}$, do not fit, calc only for a half-module (symmetry), i.e. ~300 × 7 bins for a ***single-layer modular J-PET***
(can be extended to 2γ + prompt)

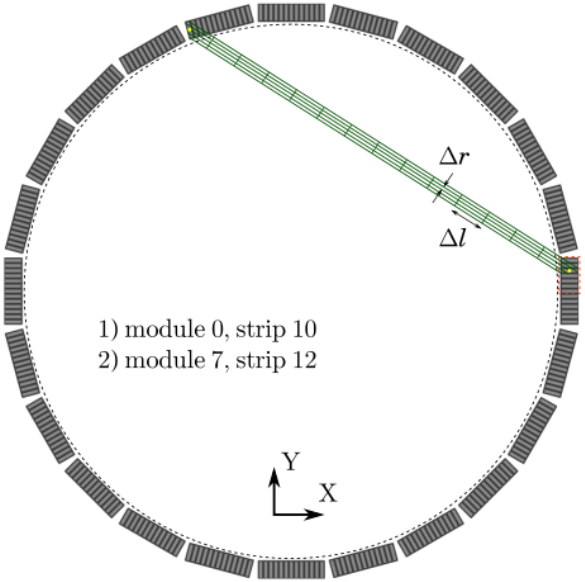

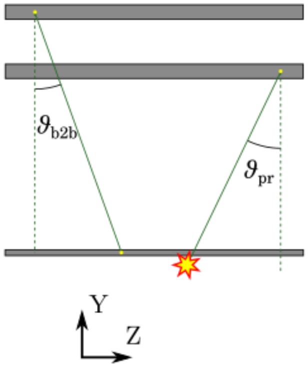

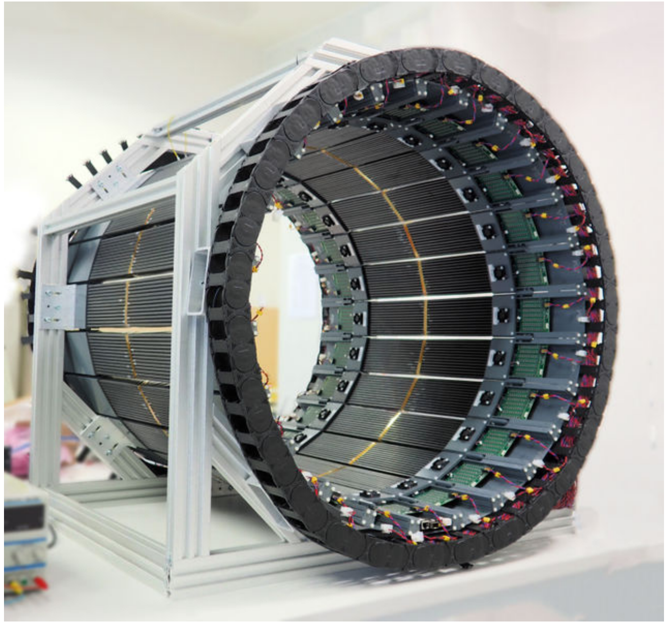

24 modules × 13 strips
(24 mm × 6 mm × 500 mm)

List-mode TOF MLEM

Add TOF: post-MC (2γ) or for each event (2γ + prompt).
Interpolate rough grid to match voxel size.

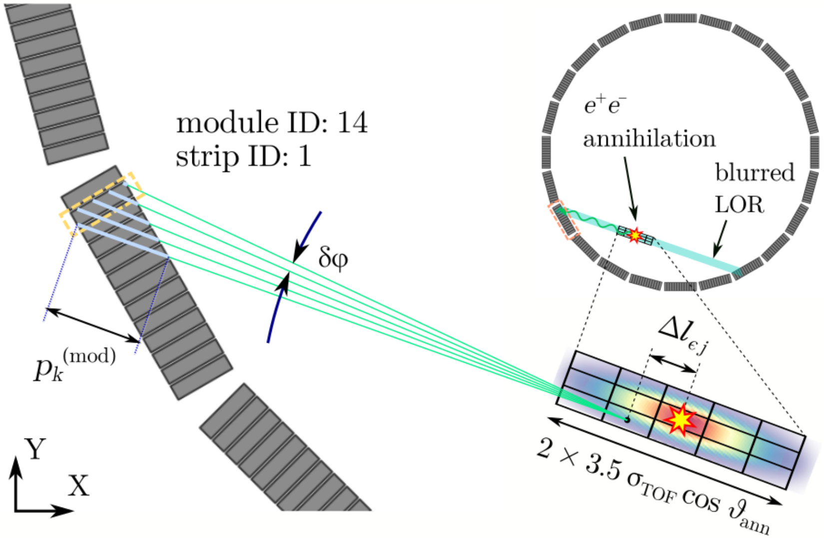

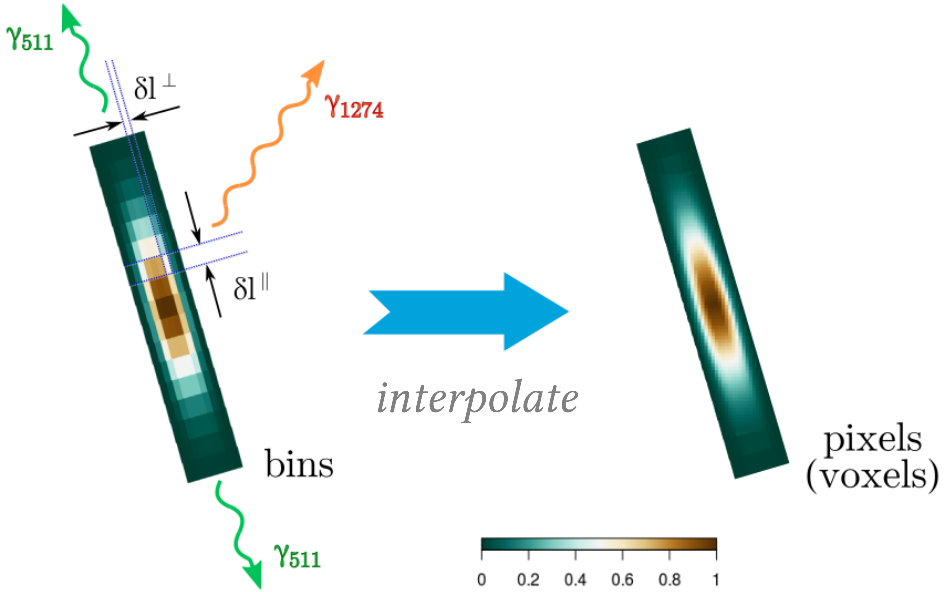

Types of coincidence data

[Kowalski P. et al. (2018) PMB]

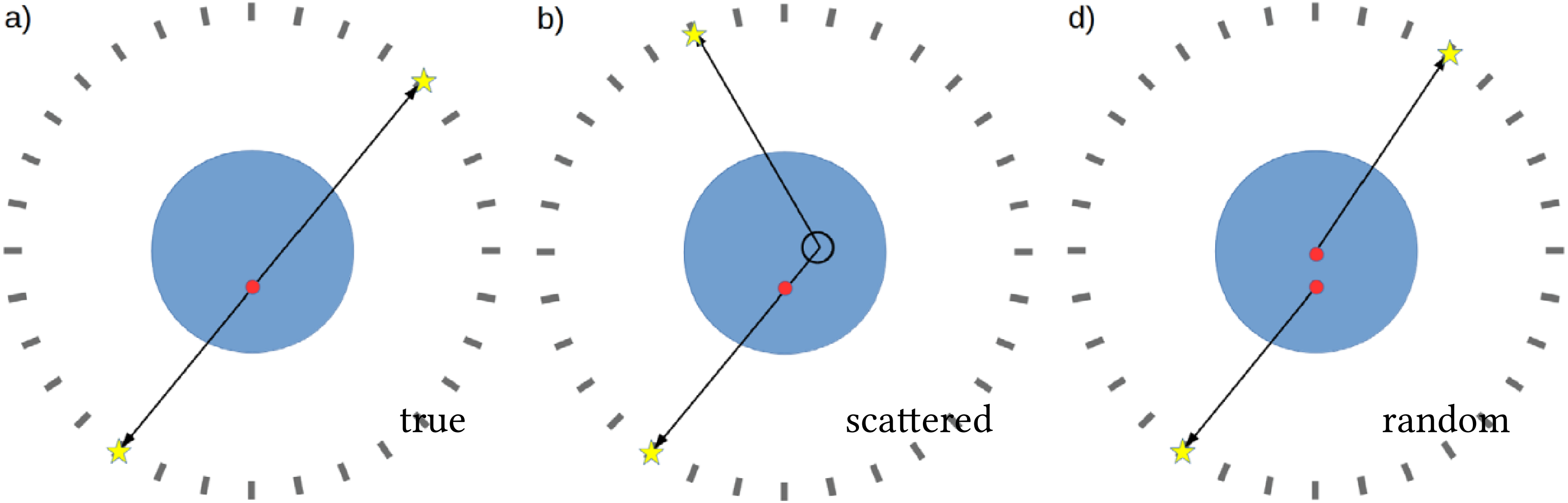

true scattered random

Single scatter simulation (SSS)

Introduced by Watson C.C. et al. (1996) – expected single Compton scattered events for a detector pair (A,B), no TOF

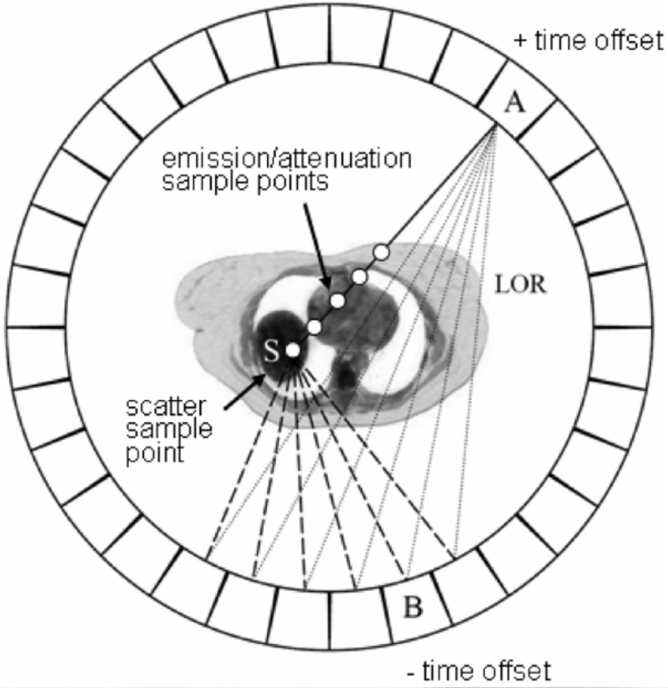

attenuation

$$S^{AB} = \int_{V_s} dV_s \left(\frac{\sigma_{AS}\sigma_{BS}}{4\pi R_{AS}^2 R_{BS}^2} \right) \frac{\mu}{\sigma_c} \frac{d\sigma_c}{d\Omega} \left[I^A + I^B \right]$$

$$I^A = \varepsilon_{AS}\varepsilon'_{BS} e^{-\left(\int_S^A \mu ds + \int_S^B \mu' ds\right)} \int_S^A \lambda(s) ds$$

activity

$$I^B = \varepsilon_{BS}\varepsilon'_{AS} e^{-\left(\int_S^A \mu' ds + \int_S^B \mu ds\right)} \int_S^B \lambda(s) ds.$$

Referring to Fig. 1, V_s is the total scatter volume (that is, the entire volume of finite density), S is the scatter point, dV_s is an incremental volume element at S, s is the distance from the scatter point along a ray such as AS, σ_{AS} is the geometrical cross section of detector A for γ-rays incident along AS, R_{AS} is the distance from S to A, ε_{AS} is the efficiency of detector A for γ-rays incident along AS, μ is the linear attenuation coefficient, λ is the emitter density in the object, σ_c is the total Compton interaction cross section, and Ω is the scattering solid angle.

STIR implementation of SSS

STIR – Software for Tomographic Image Reconstruction, current version 6.0.

Two options:

```
> simulate_scatter simulate_scatter.par
> estimate_scatter scatter_estimate.par
```

We use non-TOF **simulate_scatter**: easier for J-PET
Computationally expensive – requires downsampling
and low-res activity & attenuation images.

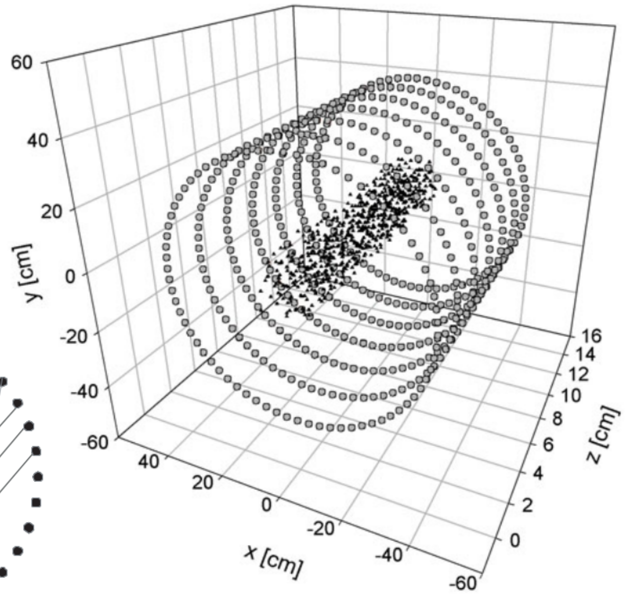

Example: use sampled
low-res bins and interpolate
[Werling A. et al. (2002)]

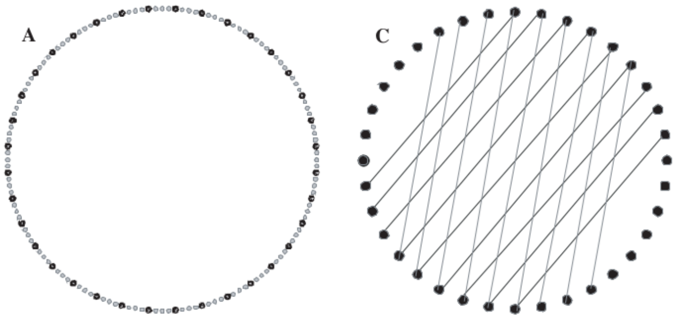

Template for SSS sinogram in STIR

Ideal cylinder, D = 73.8 cm, 24 axial 2-cm rings, 96 detectors per ring

Energy cuts: 425 keV – 650 keV

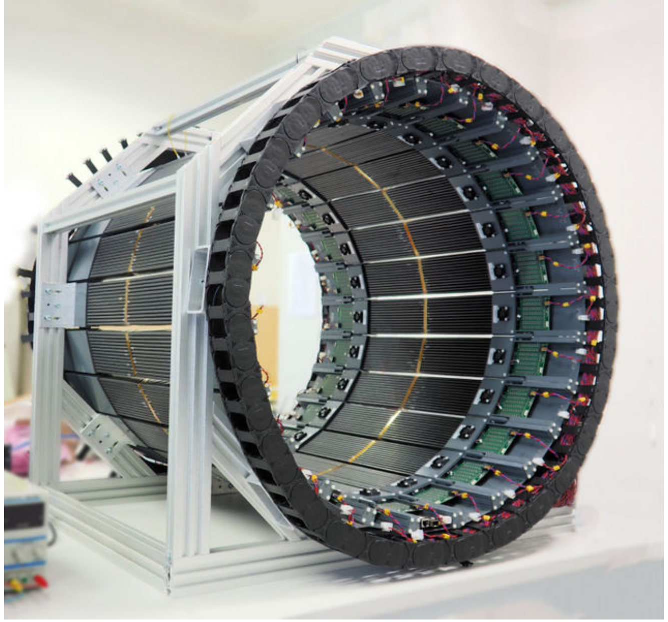

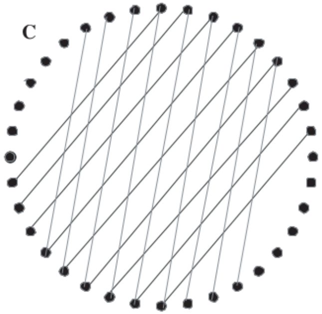

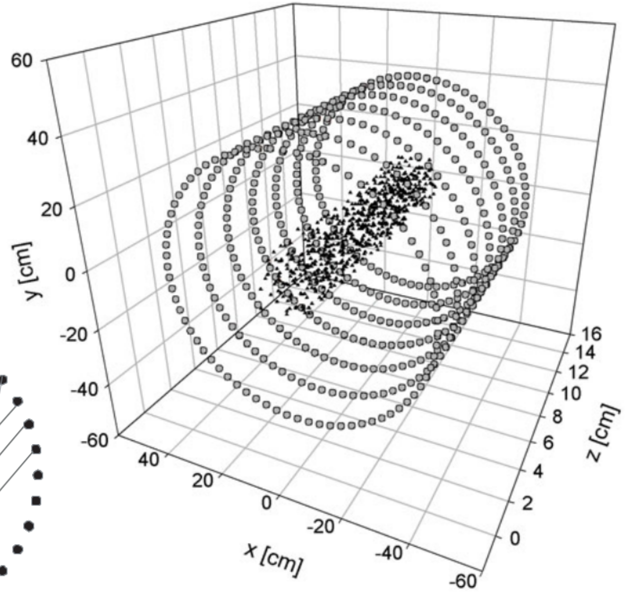

Workflow

(no randoms):

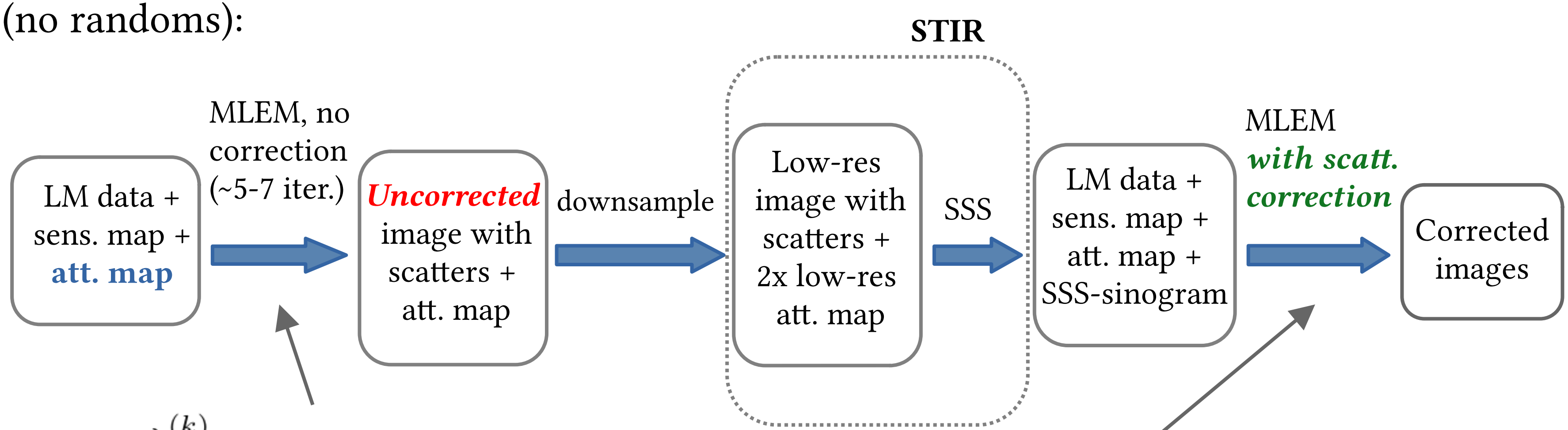

$$\lambda_j^{(k+1)} = \frac{\lambda_j^{(k)}}{\sum\limits_{i \in \mathcal{I}} a_i \chi_{ij}} \sum_{\epsilon \in \mathcal{E}} \frac{\chi(it)_{\epsilon,j}}{\sum\limits_{j' \in \mathcal{J}_\epsilon} \chi(it)_{\epsilon,j'} \lambda_{j'}^{(k)}}.$$

$$\lambda_j^{(k+1)} = \frac{\lambda_j^{(k)}}{\sum\limits_{i \in \mathcal{I}} a_i \chi_{ij}} \sum_{\epsilon \in \mathcal{E}} \frac{\chi(it)_{\epsilon,j}}{\sum\limits_{j' \in \mathcal{J}_\epsilon} \chi(it)_{\epsilon,j'} \left(\lambda_{j'}^{(k)} + \beta \cdot s_{i_\epsilon}^{(\mathrm{SSS})} / a_{i_\epsilon}\right)}.$$

Factors $s_{ie}^{(\mathrm{SSS})}$ and a_{ie} are calculated ***for each event*** (using ***interpolation*** for SSS sinogram)

Normalisation problem

$$\lambda_j^{(k+1)} = \frac{\lambda_j^{(k)}}{\sum_{i\in\mathcal{I}} n_i^{\text{cal}} a_i \chi_{ij}} \sum_{\epsilon\in\mathcal{E}} \frac{\chi(it)_{\epsilon,j}}{\sum_{j'\in\mathcal{J}_\epsilon} \chi(it)_{\epsilon,j'} \lambda_{j'}^{(k)} + \hat{b}_{i_\epsilon}^*}.$$

$$\hat{b}_{i_\epsilon}^* = (\cancel{\hat{r}_{i_\epsilon}} + \hat{s}_{i_\epsilon})/(n_{i_\epsilon}^{\text{cal}} a_{i_\epsilon})$$

Important: ignore randoms!

STIR uses ***tail-fitting*** for normalisation of SSS-sinograms (as projection data).
Difficult to apply to list-mode TOF data of J-PET.

$$\hat{s}_{i_\epsilon} \to n^{(\text{SSS})} \cdot s_{i_\epsilon}^{(\text{SSS})}$$

Current solution – normalise by each event by an ***adjustable regularisation factor*** β.

$$n_\epsilon^{(\text{SSS})} = \beta \cdot n_{\chi_\epsilon} \equiv \beta \cdot \sum_{j\in\mathcal{J}_\epsilon} \chi_{it,j}$$

$$\lambda_j^{(k+1)} = \frac{\lambda_j^{(k)}}{\sum_{i\in\mathcal{I}} a_i \chi_{ij}} \sum_{\epsilon\in\mathcal{E}} \frac{\chi(it)_{\epsilon,j}}{\sum_{j'\in\mathcal{J}_\epsilon} \chi(it)_{\epsilon,j'} (\lambda_{j'}^{(k)} + \beta \cdot s_{i_\epsilon}^{(\text{SSS})}/a_{i_\epsilon})}.$$

Scan setup

“Patient 10”:
F, 49 y.o., multifocal gastric neuroendocrine neoplasm tumour (NET G1, Ki67 2 percent)

Stats:
Ga-68-DOTATATE 158 MBq, 59 min wait,
20 min PET/CT scan (Biograph 64),
10 min scan (J-PET)

2γ data: 5.36M events;
2γ + prompt: 17.1k events (that’s why ^{68}Ga)
(too few for Ps imaging!!!)

Attenuation map (511 keV, cm^{-1})

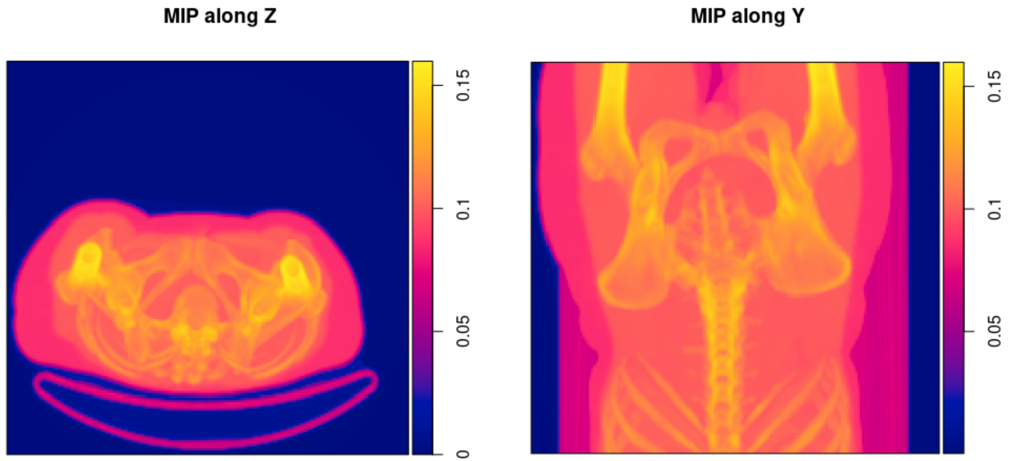

Can ignore motion here

After *geometrical pre-filtering* (2γ): ~ 3.7M coincidences

CT to the attenuation map – based on the work [Jonathan P. J. Carney, Med Phys 2006] + isocentres adjusted to match PET scan *(**some ML techniques** by Manish Das, J-PET collaboration)*

Results

SSS sinograms

Max value = 3.231525

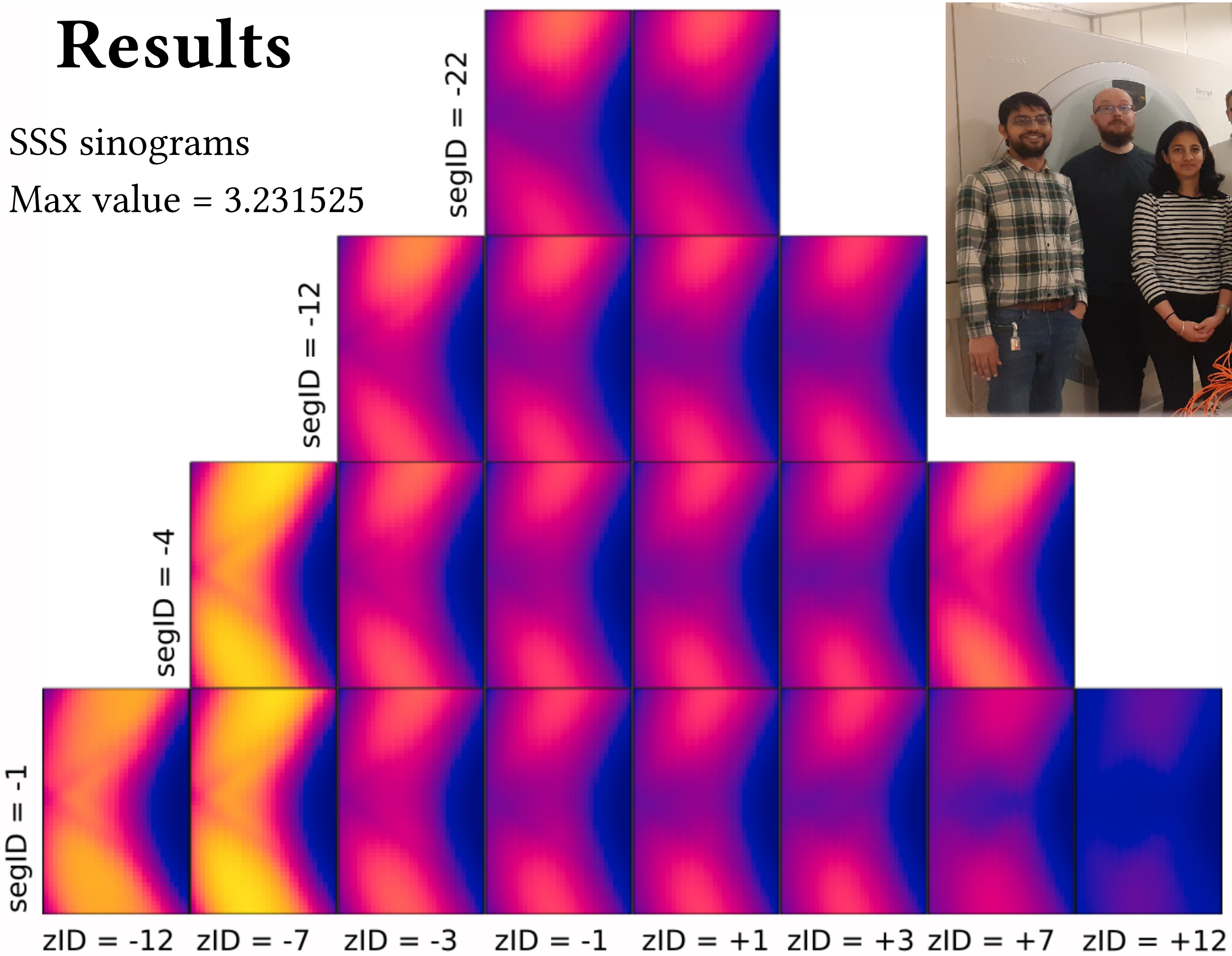

J-PET group photo at the Medical University of Warsaw

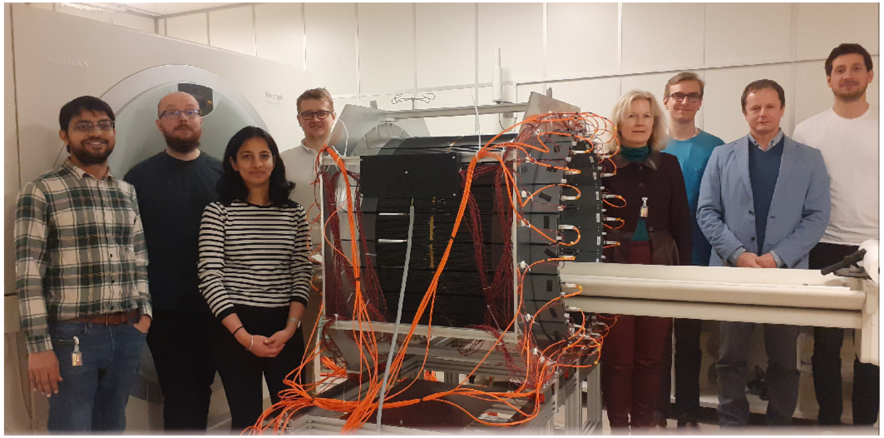

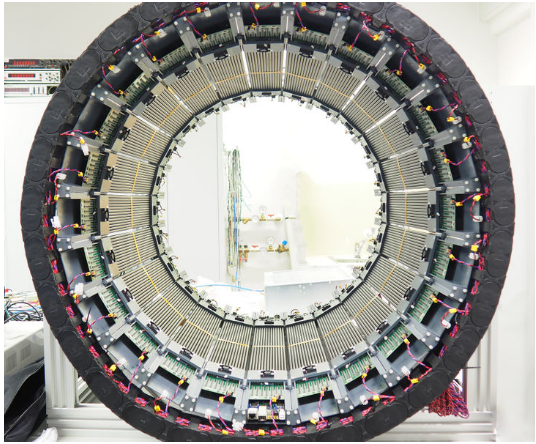

Results

Uncorrected image, maximum intensity projection (MIP)

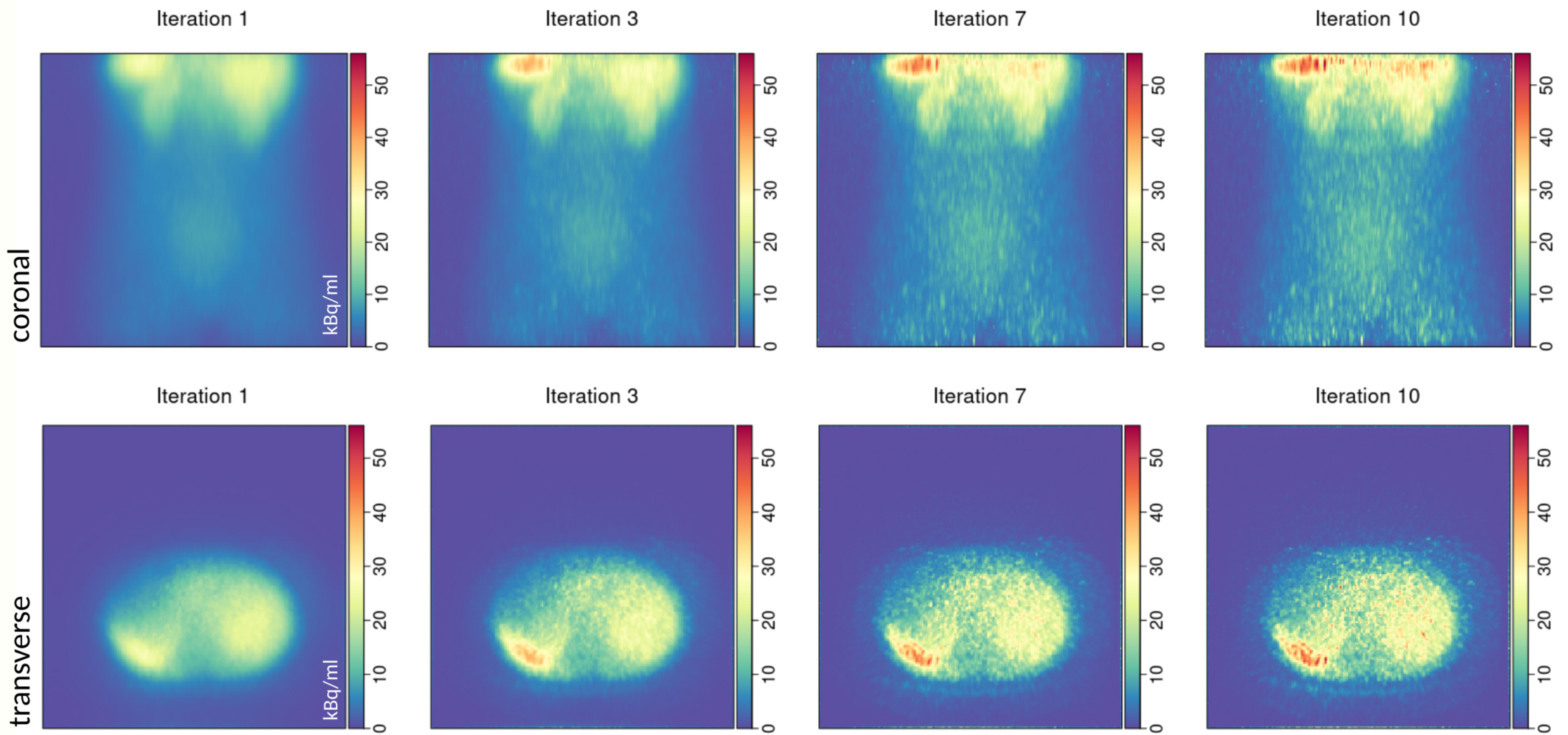

Results

Iteration 7

No correction,

Cross-sections

And MIPs

Axial smearing

in J-PET is seen

(FWHM ~ 1.5–2 cm)

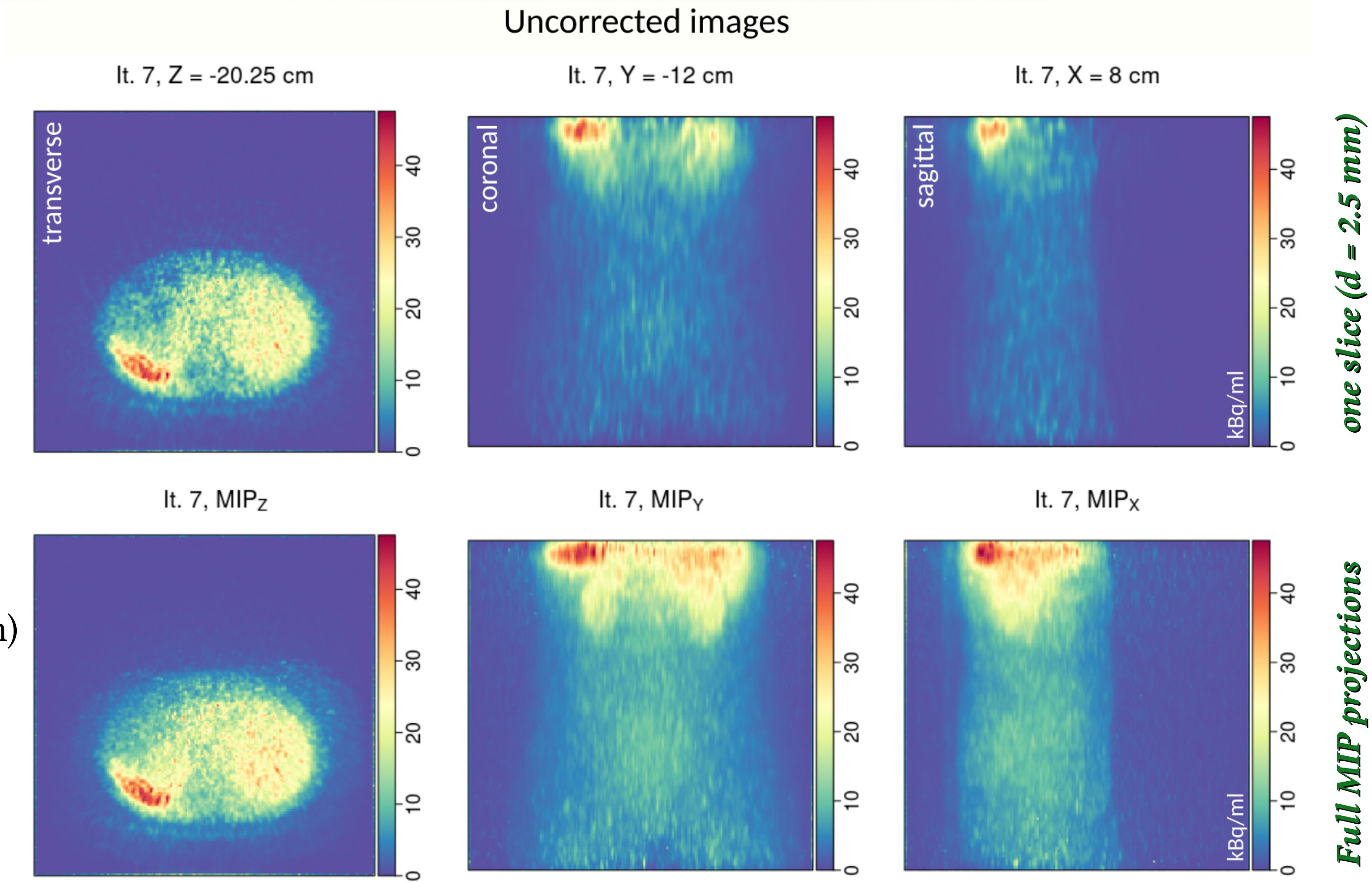

Results

Iteration 7

SSS correction,

Optimal norm:

$\beta = 0.0025$

With SSS applied

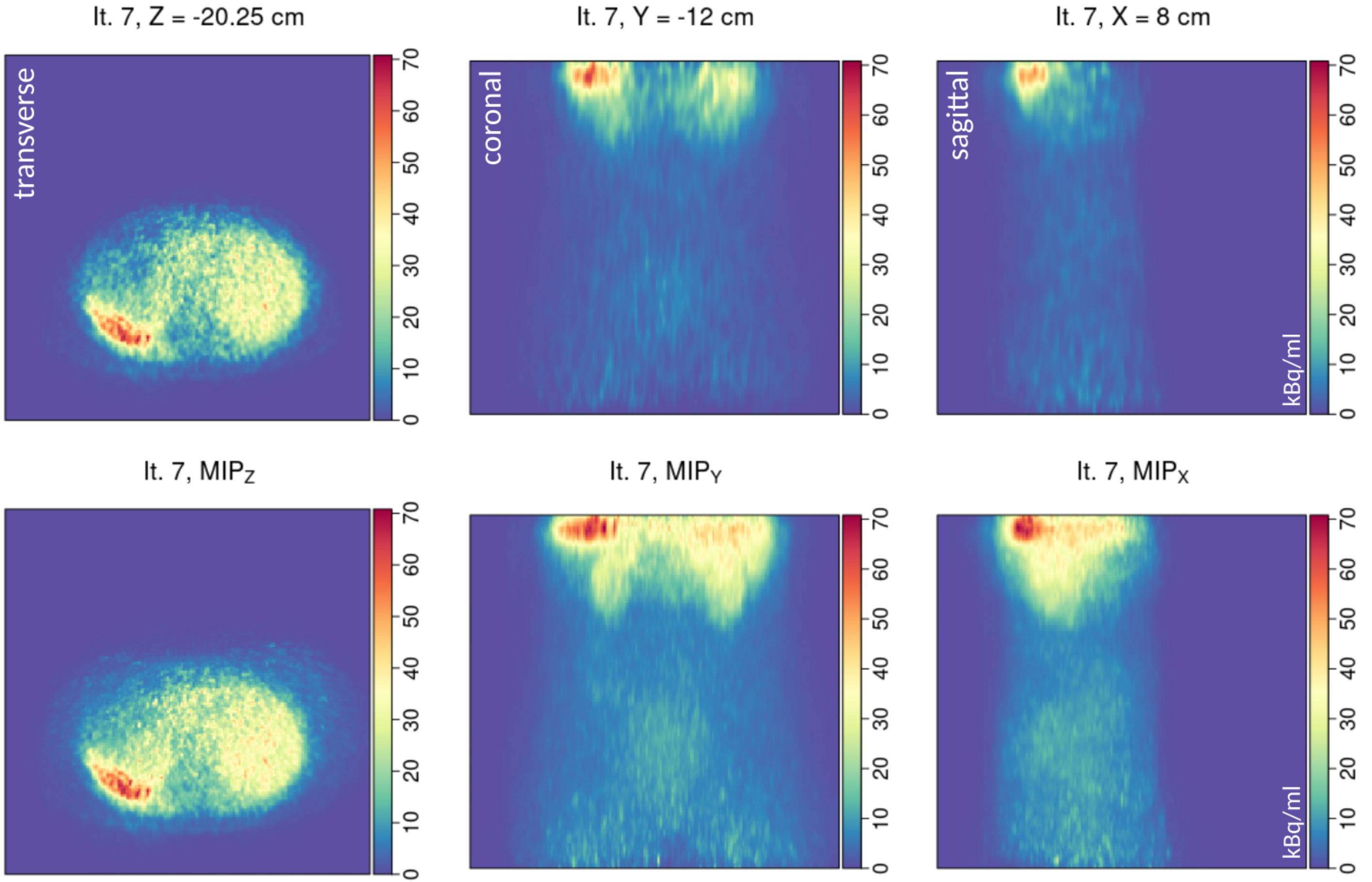

one slice (d = 2.5 mm)

Full MIP projections

Results

Iteration 7

SSS correction + Anisotropic Median-Diffusion

[Jian Ling et al. IEEE TMI (2002)] ***+***

Finite-impluse-response median hybrid filter (AMD-FMH)

[Shopa R, RAP proc, 2021]

MLEM converges!

With SSS and regularisation (AMD-FMH)

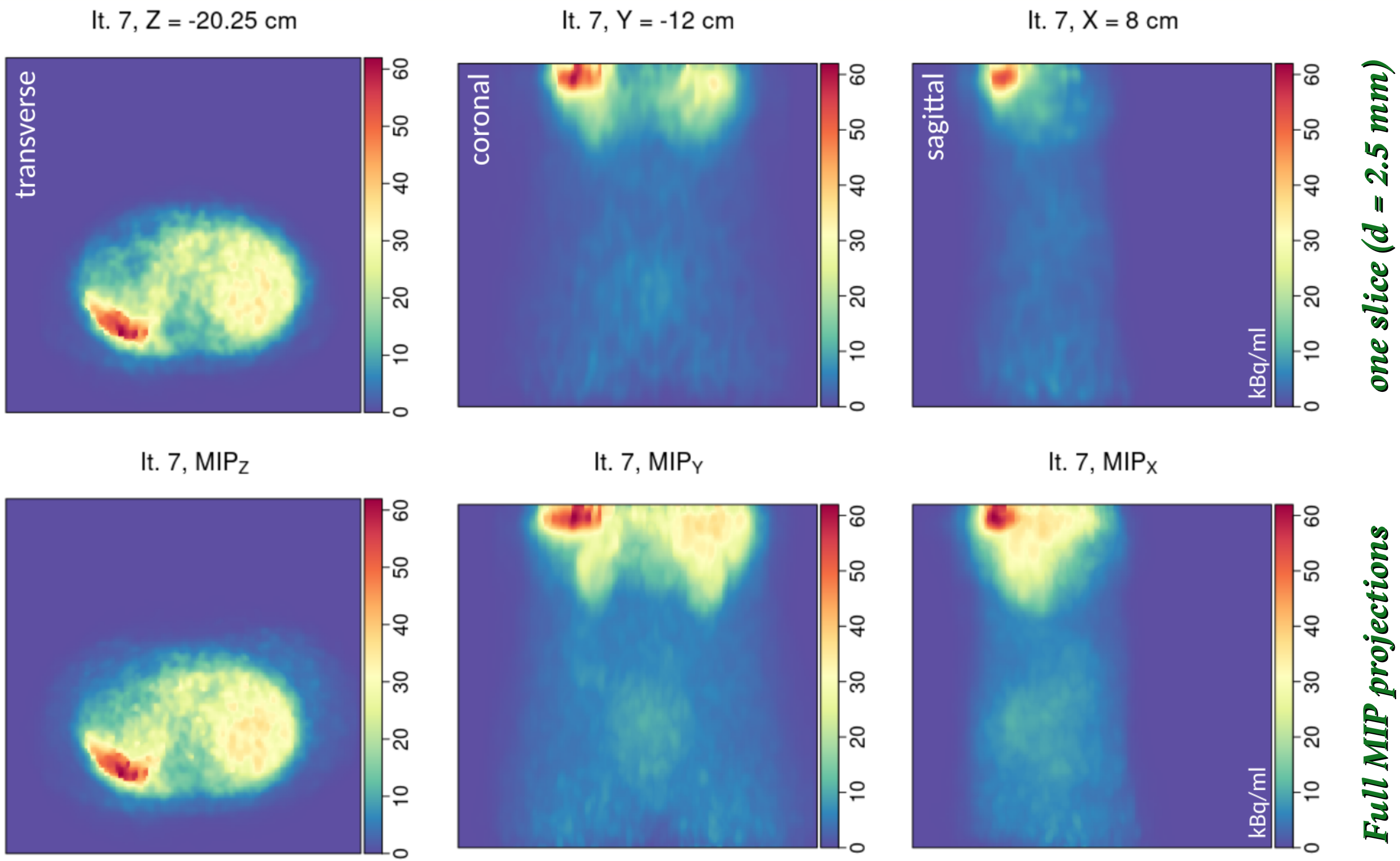

Results

Iteration 7

Direct comparison: no correction vs SSS+AMD-FMH

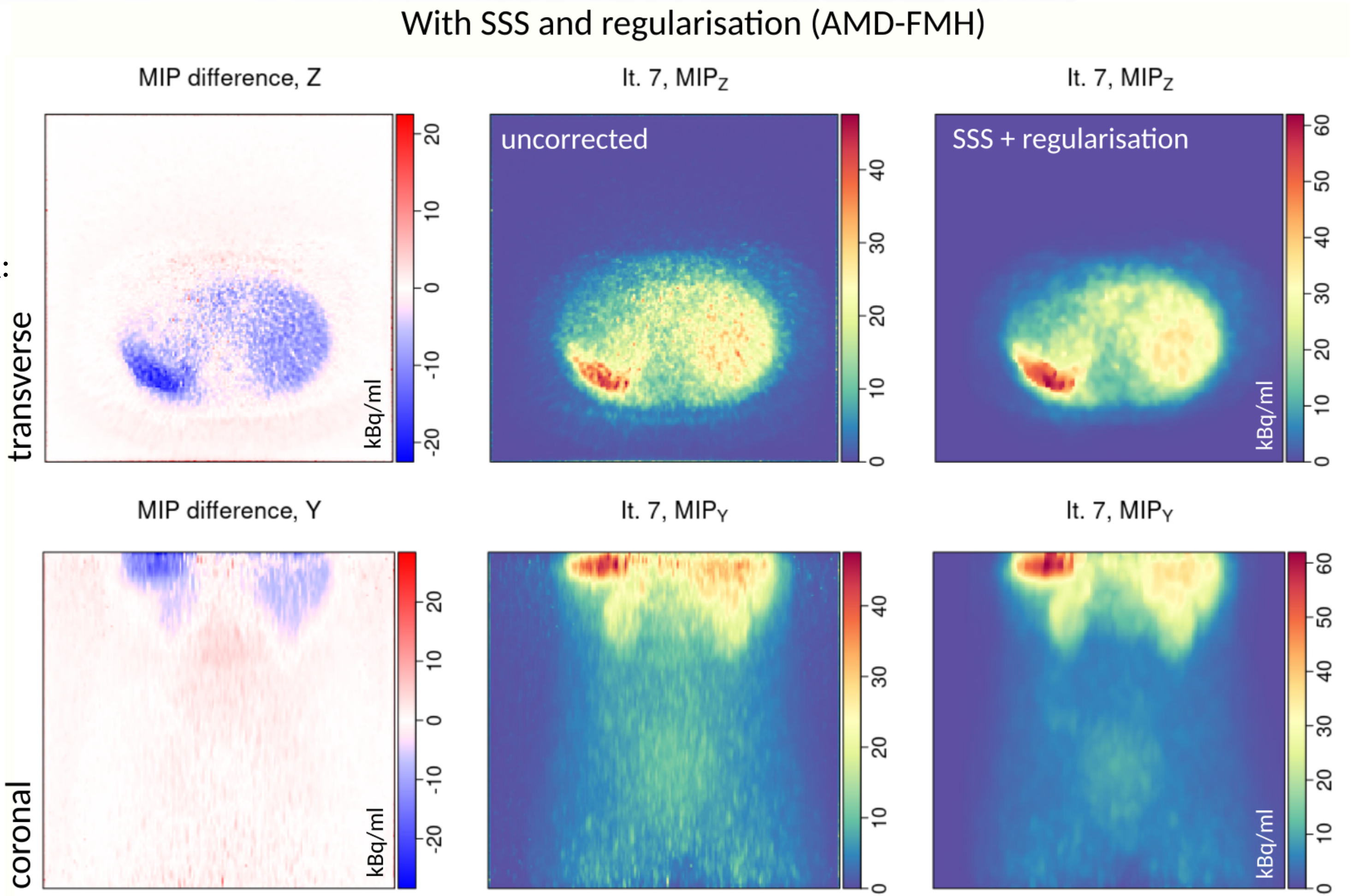

There are still ways to improve imaging!

Ways to improve

– Test data selection using ML (ongoing studies lead by Konrad Klimaszewski)

– Dedicated measurements with ^{18}F or ^{22}Na (negligible *positron range*) or account for $\mathbf{M}_{\mathbf{ps.rng}}$

$$\mathbf{M} = \underline{\mathbf{M}_{\mathrm{norm}}}\,\underline{\mathbf{M}_{\mathrm{det.res}}}\,\underline{\mathbf{M}_{\mathrm{att}}}\,\underline{\mathbf{M}_{\mathrm{Radon}}}\,\underline{\mathbf{M}_{\mathrm{ps.rng}}}$$

– Longer scans, longer FOV, proper Ps imaging

Preliminary PI for selected regions

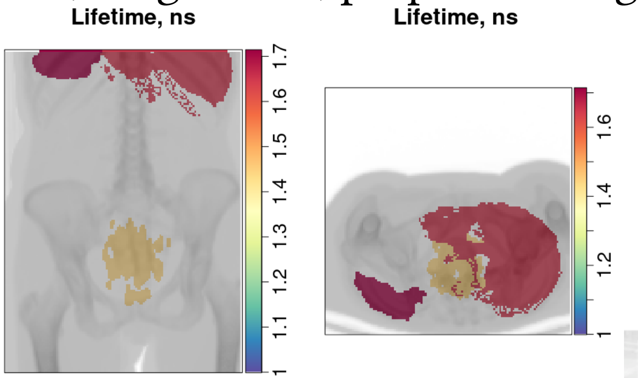

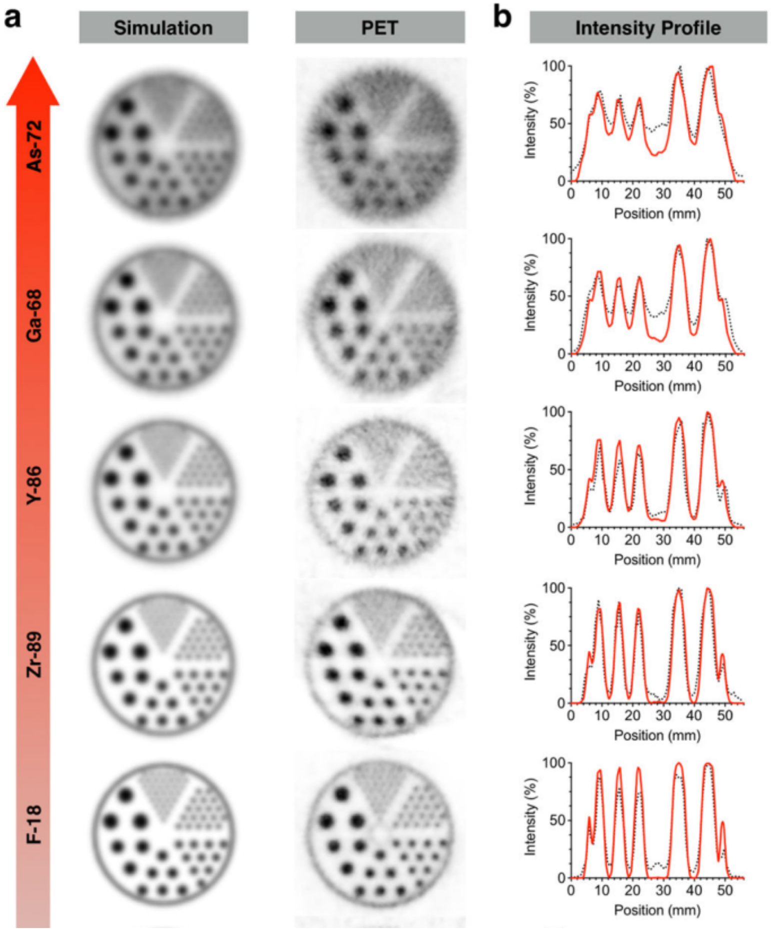

[Carter et al Mol. Imag. Biol. 2020]

Conclusions

– The first static clinical PET image acquired for the modular J-PET

– Realistic system matrix modelling that accounts for detector resolution is better than traditional PSF (e.g. in STIR or CASToR)

– Scatter correction introduced for the first time in the J-PET experiments, some issues with the normalisation yet to be resolved

– Regularisation by AMD-FHM further improves PET image as MLEM converges

– Ga-68-DOTATATE radiotracer can provide information on the positronium lifetime

– Still significant positron range to be resolved in the future

Thank You for Your attention!

NATIONAL
CENTRE
FOR NUCLEAR
RESEARCH
ŚWIERK

Template header for SSS sinogram

```
!INTERFILE  :=
!imaging modality := PT
name of data file := sss_djpet50_updAct_p10.s
originating system := unknown
!version of keys := STIR6.0
!GENERAL DATA :=
!GENERAL IMAGE DATA :=
!type of data := PET
patient orientation := head_in
patient rotation := supine
imagedata byte order := LITTLEENDIAN
number of radionuclides := 1
radionuclide name[1] := ^18^Fluorine
radionuclide halflife (sec)[1] := 6584.04
radionuclide branching factor[1] := 0.9686
!PET STUDY (General) :=
!PET data type := Emission
applied corrections := {None}
!number format := float
!number of bytes per pixel := 4
number of dimensions := 4
matrix axis label [4] := segment
!matrix size [4] := 47
matrix axis label [3] := view
!matrix size [3] := 48
matrix axis label [2] := axial coordinate
!matrix size [2] := { 1,2,3,4,5,6,7,8,9,10,11,12,13,14,15,16,17,18,19,20,21,22,23,24,23,22,21,20,19,18,17,16,15,14,13,12,11,10,9,8,7,6,5,4,3,2,1}
matrix axis label [1] := tangential coordinate
!matrix size [1] := 31
minimum ring difference per segment :=
{ -23,-22,-21,-20,-19,-18,-17,-16,-15,-14,-13,-12,-11,-10,-9,-8,-7,-6,-5,-4,-3,-2,-1,0,1,2,3,4,5,6,7,8,9,10,11,12,13,14,15,16,17,18,19,20,21,22,23}
maximum ring difference per segment :=
{ -23,-22,-21,-20,-19,-18,-17,-16,-15,-14,-13,-12,-11,-10,-9,-8,-7,-6,-5,-4,-3,-2,-1,0,1,2,3,4,5,6,7,8,9,10,11,12,13,14,15,16,17,18,19,20,21,22,23}
Scanner parameters:=
  Scanner type := unknown
  Number of rings                          := 24
  Number of detectors per ring             := 96
  Inner ring diameter (cm)                 := 73.872
  Average depth of interaction (cm)        := 0.01
  Distance between rings (cm)              := 2
  Default bin size (cm)                    := -1
  View offset (degrees)                    := 0
  Maximum number of non-arc-corrected bins := 31
  Default number of arc-corrected bins     := 0
```

What if other isotope?

Simple cylindrical geometry

Template header for SSS sinogram

```
Scanner parameters:=
  Scanner type := unknown
  Number of rings                          := 24
  Number of detectors per ring             := 96
  Inner ring diameter (cm)                 := 73.872
  Average depth of interaction (cm)        := 0.01
  Distance between rings (cm)              := 2
  Default bin size (cm)                    := -1
  View offset (degrees)                    := 0
  Maximum number of non-arc-corrected bins := 31
  Default number of arc-corrected bins     := 0
  Energy resolution            := 0.16
  Reference energy (in keV) := 511
  Number of blocks per bucket in transaxial direction         := 0
  Number of blocks per bucket in axial direction              := 0
  Number of crystals per block in axial direction             := 0
  Number of crystals per block in transaxial direction        := 0
  Number of detector layers                                   := 1
  Number of crystals per singles unit in axial direction      := -1
  Number of crystals per singles unit in transaxial direction := -1
  Scanner geometry (BlocksOnCylindrical/Cylindrical/Generic)  := Cylindrical
End scanner parameters:=
number of time frames := 1
number of energy windows := 1
energy window lower level[1] := 425
energy window upper level[1] :=  650
start vertical bed position (mm) := 0
start horizontal bed position (mm) := 0
!END OF INTERFILE :=
```

Energy cuts

Tangential: s
Axial: Z
View: ϕ
Segment: θ

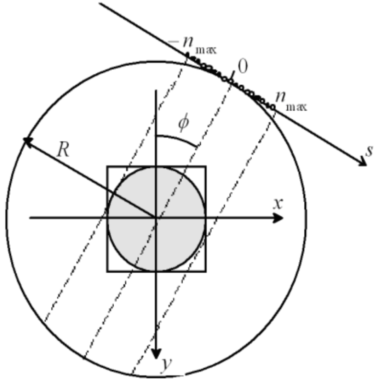

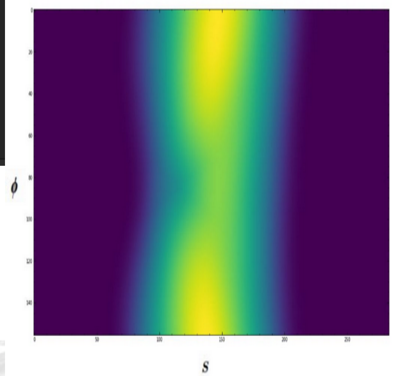

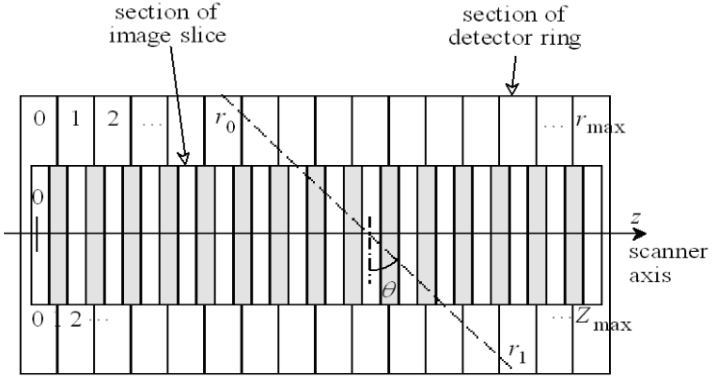

Single scatter simulation (SSS)

Courtesy of Jakub Baran

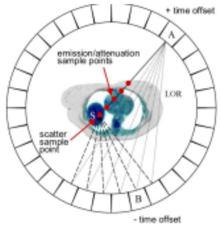

Fig. 1. The single scatter simulation model.

Conventional non-TOF PET

Determined from preliminary estimated emission and transmission image volumes

Linear attenuation coefficient

Total Compton interaction cross section

Emitter density in the object

$$S^{AB} = \int_{V_s} dV_s \left(\frac{\sigma_{AS}\sigma_{BS}}{4\pi R_{AS}^2 R_{BS}^2} \right) \frac{\mu}{\sigma_c}\frac{d\sigma_c}{d\Omega}\left[I^A + I^B\right]$$

$$I^A = \varepsilon_{AS}\varepsilon'_{BS}\, e^{-\left(\int_S^A \mu ds + \int_S^B \mu' ds\right)} \int_S^A \lambda(s)\, ds$$

$$I^B = \varepsilon_{BS}\varepsilon'_{AS}\, e^{-\left(\int_S^A \mu' ds + \int_S^B \mu ds\right)} \int_S^B \lambda(s)\, ds$$

Scattering solid angle

Scatter volume

Scatter point

Distance from S to A

Efficiency of detector A for γ-rays incident along AS*

Distance from the scatter point along a ray such as AS

Geometrical cross section of detector A for γ-rays incident along AS

Calculated from Klein-Nishina formula

*Primed quantities are evaluated at the scattered photon's energy, while unprimed ones are evaluated at 511 keV.